Int. J. Nano Dimens., 11 (4): 364-376, Autumn 2020

ORIGINAL ARTICLE

Rapid and sensitive electrochemical detection of DNA with Silver nanoparticle dispersed poly (9, 9-dioctylfluorene-ran-phenylene) nanocomposites

Pangajam Annamalai [1], Dinakaran Kannaiyan [1*], Harichandran Gurusamy [2]

1 Department of Chemistry, Thiruvalluvar University, Vellore – 632 115, India
2 Department of Polymer Science, University of Madras, Guindy Campus, Chennai-600025, India

Received 14 Appril 2020; revised 07 September 2020; accepted 10 September 2020; available online 11 September 2020

Abstract

In this study a sensitive electrochemical sensor for the detection of *E.coli* has been developed using silver nanoparticle (Ag) embedded poly (9, 9-dioctylfluorene-ran-phenylene) (CFP) nanocomposite as a conductive platform and DNA hybridization technique. The new polymer was synthesized from 9, 9-dioctylfluorene and 1, 3-dichlorobenzene and biphenyl through Friedel Crafts alkylation reaction and the synthesized polymer as well as the Ag nanoparticles loaded composite were characterized using Fourier-transform infrared spectroscopy (FTIR), Nuclear Magnetic Resonance (NMR), X-ray powder diffraction (XRD), Scanning Electron Microscopy (SEM) and Transmission Electron Microscopy (TEM) analysis. For accurate and rapid label-free electrochemical detection of pathogenic bacteria such as *E.coli*was studied by spin coating the nanocomposite suspension into indium tin oxide electrode (ITO) followed by the immobilization of aminoterminated oligonucleotide (pDNA), as probe. The resultant pDNA/Ag-CFP/ITO biosensor was then used to detect ssDNA, cleaved from genomic DNA of *E.coli*, using differential pulse voltammetry (DPV) technique. Under optimal experimental conditions, the biosensor could detect ssDNA in a wide linear range from 1×10^{-15} M to 1×10^{-22} M with a lowest detection limit of 1×10^{-22} M.

Keywords: *Conductive Nanocomposites; DPV Sesnor; E. Coli Detection; Electrochemical Sensor; Polyfluorene Derivatives.*

How to cite this article

Annamalai P., Kannaiyan D., Gurusamy H. Rapid and sensitive electrochemical detection of DNA with Silver nanoparticle dispersed poly (9, 9-dioctylfluorene-ran-phenylene) nanocomposites. Int. J. Nano Dimens., 2020; 11 (4): 364-376.

INTRODUCTION

E.coli is a member of Enterobacteriaceae, which is a bacterial family [1], found in most common intestinal microorganism of humans and warm-blooded animals [2]. Some strains of this bacterium *E. Coli* is mainly transmitted through consumption of contaminated water samples. Lack of hygiene practice in production, handling and transportation of water samples could lead to easy contamination of *E. Coli.* The increasing number of water poisoning cases due to *E. Coli* implies there is a crucial need for a more sensitive and rapid detection method to detect and quantitate the presence of this pathogen in water samples including oceans [3, 4], rivers [5, 6], lakes [7, 8] and sewer water [9, 10]. Early detection of *E. Coli* in the water will help to prevent the spread of *E. Coli* [11].

There are different tests for a pathogenic bacteria detection in clinical samples such as non- culturing and culturing methods, enzyme-linked immunosorbent assay (ELISA), polymerase chain reaction (PCR), optical detection methods [12-13] and isothermal microcalorimetry (IMC) [14]. These procedures are time-consuming, expensive and require specialist equipment and

* Corresponding Author Email: : kdinakaran@tvu.edu.in
kdinakaran.tvu@gmail.com

well-trained personnel. Therefore, development of a methodology that provides easy preparation of sample and rapid recognition of bacteria remain desirable and challenging.

Electrochemical biosensors have attracted considerable attention for its intrinsic advantages, such as simplicity, high compatibility, impressive sensitivity, portability, cost- efficiency, and quick response [15]. Furthermore, the electrochemical biosensors can tolerate matrix effects of physiological samples, and provide direct detection of bacteria in clinical samples [16]. The combined features of electrochemical techniques with high-selective nature of oligonucleotide has led to the design of biosensors for the detection of specific genomic DNA sequences. In recent years, a series of signal amplification strategies have been applied to improve the sensitivity, signal-to-noise (S/N) ratio and low detection limit of electrochemical methods [17]. This biosensor is very useful and highly desirable because of its high productivity, low limit of detection, simplicity portability and most importantly, it requires a low volume of analytes.

Conducting polymers are organic conjugated polymers that feature an extended π- orbital system through which electrons can move from one end of the polymer to the other. CPs also exhibit very high flexibility, which can be modulated together with their electrical properties by using appropriate chemical modeling and synthesis [18-20]. These distinctive properties of CPs have broadened their applications in various technological fields, such as in the design of light-emitting diodes [21], anti-static coating [22], electrochromic devices [23], solar cells [24], anti-corrosion coatings [25], chemical sensors and biosensors [26], and drug-release systems [27-28]. Poly (fluorene)s and derivatives are attracting significant interest in the context of polymer-based optoelectronic devices, and in particular for the fabrication of efficient and long-lived light-emitting diodes [29]. It provides excellent electrochemical activity and also, it can act as a suitable matrix for the immobilization of bio-components on the surface electrode [30].

Among various nanomaterials, Ag NPs are widely used in sensing fabrication due to their biocompatibility, optical, electronic, and electrochemical properties [31-33]. Excellent physicochemical attributes of silver based conducting polymers (CP) enhanced the increasing use of these materials as a component in biosensors [34]. Specifically, high electrical conductivity and enhanced surface areas of silver-based CP in combination with ssDNA as the recognition element improves the overall sensitivity of the biosensors [35]. Silver, a CP based ssDNA nanocomposite, has emerged as an attractive polymer nanocomposite in the field of electrochemical application mainly due to its excellent electrical and thermal conductivity [36-37]. Abdullah et al developed an electrochemical biosensor using silver nano prisms which exhibited a wide detection range from 0.01– 0.1 pM of *E.Coli* [38].

He et al studied multiplexed detection of DNA with conjugated polymer on Ag/Au strip nanorod [39]. David Whitten *et al*. [40] developed an assay for a target single strand DNA based on conjugated polymer fluorescence super quenching, in which an anionic poly (phenylene ethynylene) immobilized polystyrene sphere with a quencher labeled DNA has been used. In all of these reports involve tedious procedure with the usage of multiple components such as dye or quencher labeled DNA [41-42], quantum dots [43] and Au/Ag film etc., [44] In the present work we have synthesized new conducting polymer by Fridelcraft alkylation method to enhance the conductivity of the nanoparticle as shown in Scheme. 1. Ag-CFP biosensor was designed using the hybridization technique between Ag and CFP without any chemical reduction method and drop-casted onto Indium Tin Oxide (ITO). In this study, ssDNA was used as a linker to ensure the binding between Ag-CFP polymer nanocomposites. Under the optimal conditions, the biosensor could detect the *E. Coli via* differential pulse voltammetry (DPV) technique. Furthermore, the biosensor was also applied to detect the water sample pathogen in real drinking water samples. The developed biosensor has several distinct advantages including high sensitivity, good selectivity and low cost. This study is the first to report the application of ssDNA/Ag-CFP/ITO as a biosensor for detecting *E. Coli.*

EXPERIMENTAL

Materials and reagents

1, 3- dichlorobenzene, 1-1’ biphenyl, 9, 9-dioctyl-9H-fluorene, dichloromethane (DCM) were of analytical grade and purchased from SRL and Fischer scientific, India. The disodium hydrogen phosphate (Na_2HPO_4), potassium dihydrogen

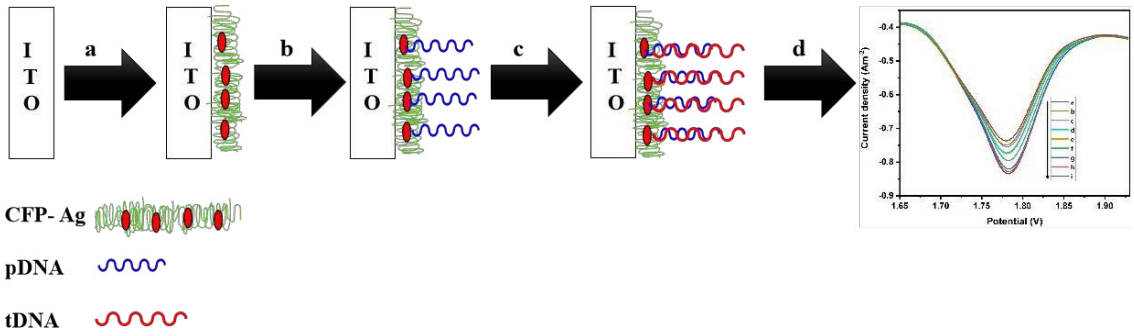

Fig. 1. A schematic diagram of the modification process of ITO. (a) drop casting of Ag-CFP on ITO, (b) pDNA immobilization on Ag -CFP/ITO surface, (c) Ag - CFP/pDNAincubated with the tDNA and (d) DPV measurements.

phosphate (KH_2PO_4), sodium chloride (NaCl) and potassium chloride (KCl) were purchased from Sigma-Aldrich. All chemicals and solvents were obtained from the commercial sources and used directly without further purification, and all glass wares were cleaned successively with aqua regia and D.I water and then dried before use. Probe DNA (pDNA): amine-5'-GGT CCG CTT GCT CTC GC-3' and the genomic DNA of *E.coli* were purchased from Synergy Scientific products, India. The genomic DNA was cleaved using PCR technique, which resulted in ssDNA solution in Phosphate buffer at pH 7.0 and was stored at -20 °C prior to use.

Instrumentation

The functional groups of the CFP, Ag and were determined by Fourier transform infrared (FT-IR), whereas the ^{1}HNMR analysis was done through Bruker instrument with 400 MHz. The morphology of the prepared nanocomposite was characterized using a Transmission Electron Microscope (FEI-TECNAI-G2 20 TWIN) and Scanning Electron Microscopy (Hitachi- S-3400N). The electrochemical experiments were performed using, an electrochemical workstation (CHI604E). Three-electrode system was used along with ITO, namely, the working electrode, a platinum wire, the counter electrode and silver/silver chloride (Ag/AgCl), the reference electrode. The ITO surface was cleaned successively with aqua regia and D.I water and then dried before use.

Synthesis of Silver nanoparticles

For the preparation of silver nanoparticles, silver nitrate solution (1.0 mM) and 8% (w/w) Sodium Dodecyl Sulphate (SDS) were used as a metal salt precursor and a stabilizing agent, respectively. Hydrazine hydrate solution (4.0 mM) and sodium citrate solution (2.0 mM) were used as reducing agents. The transparent color less solution was converted to the characteristic pale yellow and pale red color, when sodium citrate was used as stabilizing agent. The occurrence of color indicated the formations of silver nanoparticles were purified by centrifugation. To remove excess silver ions, the silver colloids were washed at least three times with deionized water under nitrogen stream [45].

Synthesis of poly (9, 9-dioctylfluorene-ran-phenylene)

In a 250 mL round bottom flask 6 mmol of 9, 9-dioctyl-9H-fluorene, 4mmol of 1,3-dichlorobenzene and 4 mmol 1,1'-biphenylwas added 100 mL of dichloromethane (DCM), and 4.00 g of anhydrous aluminum chloride (30 mmol) were added sequentially. The reaction mixture was fitted with a condenser and heated to 70 °C for 16 h under reflux. After the reaction time, the resulting mixture was cooled to room temperature. The solid brown precipitate was filtered off, washed several times with DCM, methanol and water to completely remove the unreacted starting precursors and catalyst, and dried in a vacuum for 6 h to obtain the solvent free material with 84% yield [46].

Preparation of Ag-CFP polymer nanocomposites

1 mg, 3mg and 5mg of Ag were dispersed in 10 mL chloroform ($CHCl_3$) and ultrasonicated for 1 hour to get a suspension. Further, 0.2g of CFP was added in $CHCl_3$ solution followed by ultrasonication for 30 minutes which resulted in Ag-CFP polymer nanocomposite formation.

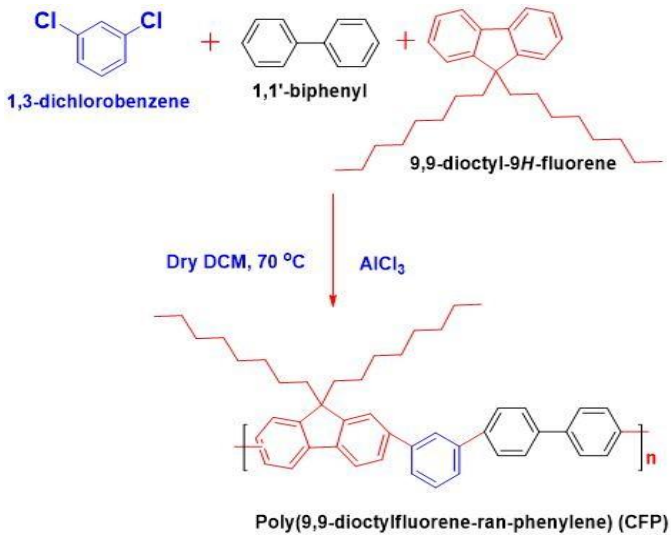

Fig. 2. Synthesis of poly (9, 9-dioctyl fluorene-ran-phenylene).

Fabrication of the pDNA/Ag-CFP/ITO biosensor electrode and sensing studies

ITO was initially polished using 0.05 µm-sized alumina fine powder to remove impurities from the electrode surface, and the electrode was then ultrasonicated, rinsed with distilled water and then left to dry at room temperature. Ag-CFP solution was spin coated onto ITO to obtain Ag-CFP/ITO electrodes. The thickness of the prepared composted is 0.05mm.To fabricate the sensing electrode of pDNA/Ag-CFP/ITO biosensor, firstly, the Ag- CFP/ITO was immersed into pDNA solution (oligonucleotide complementary to ssDNA of *E.coli*) with a concentration of 10 µmol L^{-1} for 30 min, then removed and left to dry under ambient conditions. The fabricated electrode was then stored at 4 °C until future use. The overall detection process is schematically shown in Fig. 1. Further, the pDNA/Ag-CFP/ITO was immersed into tDNA solution (ssDNA cleaved from genomic DNA of *E.coli)* having varying concentrations for 30 min, then removed and washed with DD water, and air dried at room temperature to obtain pDNA-tDNA/ Ag-CFP/ITO for DPV analysis.

RESULTS AND DISCUSSION

The Fig. 2 presents the synthesis of poly (9, 9-dioctylfluorene-ran-phenylene), a random copolymer of fluorine and phenylene units using Friedel Crafts alkylation reaction. The phenylene units are linked as 1,3 and 1,4 position of benzene and biphenyl moieties.

FT-IR Studies

FTIR spectra of Ag, Ag loaded CFP has been given in Fig. 3. FTIR spectra of Ag nanoparticles exhibited prominent peaks at 590 cm^{-1} and 1353 cm^{-1} thereby corresponding to Ag-Ag and Ag-O bonds, respectively [47-48]. The FTIR spectrum of CFP C-H stretching frequency appeared at 2970 cm^{-1}, C-C stretching frequency appeared at 1611 cm^{-1} and the C-H bending frequency appeared at 1254 cm^{-1}. The FTIR spectrum of polymer nanocomposite having various weight percentage of Ag shows the aromatic C-H stretching vibration at 2965, 2926 and 2910 cm^{-1} and C-H bending vibration at 1245, 1215, and 1202 cm^{-1} for 1%, 3% and 5% of Ag-CFP, respectively.The IR absorption due to C-C stretching is appeared at 1602, 1595 and 1582 $cm^{-1}$and the metal oxide peak present in Ag-CFP is appeared at 588, 604, 616 $cm^{-1}$for 1%, 3% and 5% of Ag-CFP polymer nanocomposites, respectively.

^{1}HNMR Studies

Fig. 4 shows the ^{1}H-NMR spectrum of CFP base in $CDCl_3$. The CFP polymer exhibits the

strongest medium of broad peak centered at 7.032 to 7.601 ppm (m) due to protons fluorene and phenyl units, the sharp peak centered at 1.035 to 4.085ppm (m) is due to the protons of aliphatic chain units of the CFP.

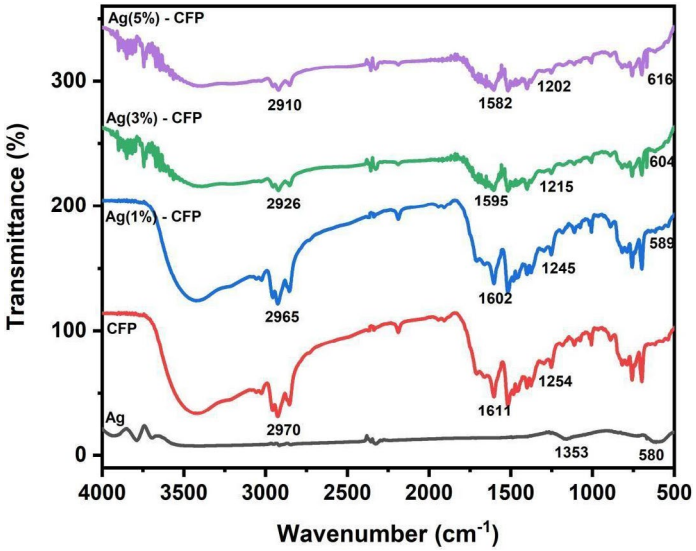

Fig. 3. FTIR spectrum of Ag, CFP, Ag (1%) - CFP, Ag (3%) - CFP, Ag (5%) – CFP.

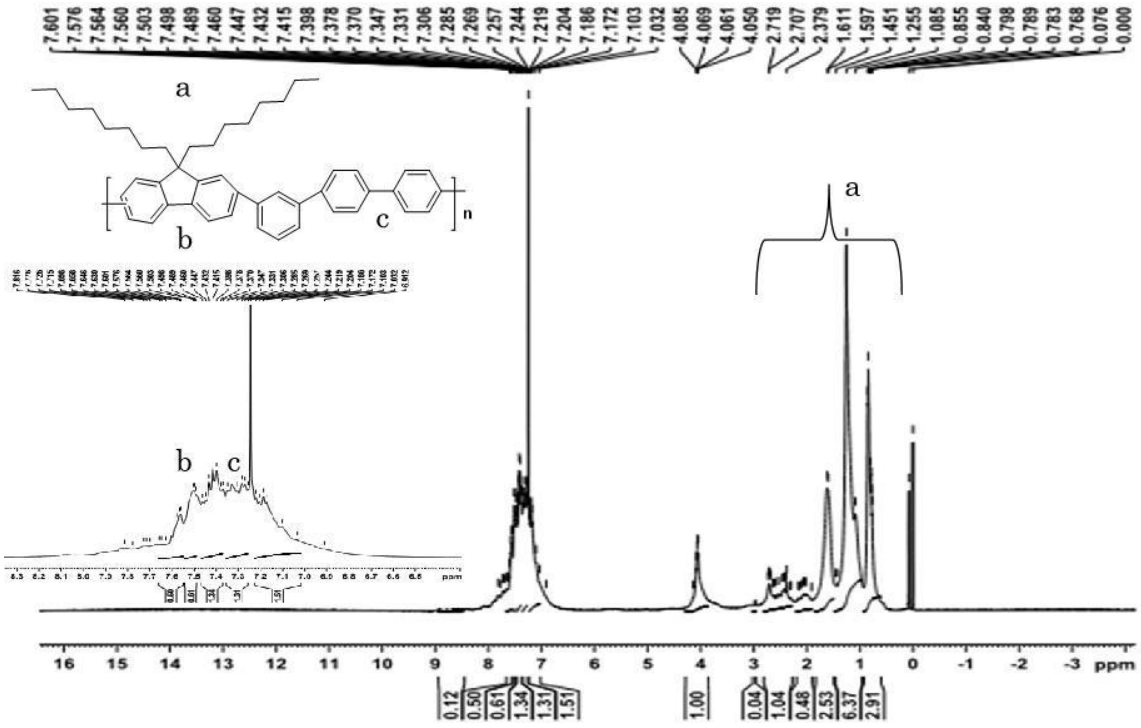

Fig. 4. ^{1}HNMR spectrum of Poly (9, 9-dioctylfluorene-ran-phenylene).

XRD Studies

The XRD patterns for Ag, CFP, Ag (1%) - CFP, Ag (3%) - CFP, Ag (5%) - CFP polymer nanocomposites are shown in Fig. 5a–e, respectively. The diffraction pattern of silver nanoparticles, presented in Fig. 5a, shows sharp and well-defined diffraction lines at 2θ = 38.1°, 44.3°, 64.2° and 77.3°, which can be assigned to the (111), (200), (220) and (311) reflections of the face centered cubic (fcc) structure of metallic silver, respectively [49]. The lattice parameter calculated from XRD pattern is a=b=c=4.079 A° in agreement with the literature

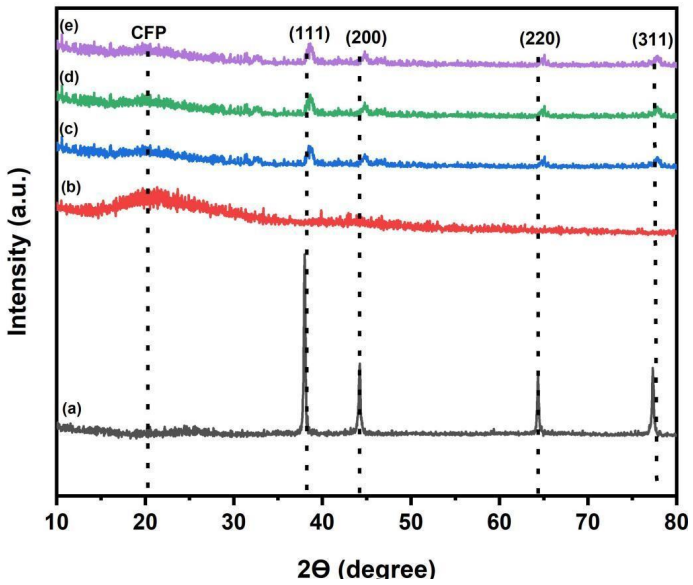

Fig. 5. XRD patterns for (a) Ag, (b) CFP, (c) Ag (1%) - CFP, (d) Ag (3%) - CFP, (e) Ag (5%) - CFP polymer nanocomposite.

Table.1. XRD parameters of Ag-CFP nanocomposites.

Sample	FWHM β (°)	Crystalline Size D(nm)	Dislocation density $\delta \times 10^{-3} (nm^{-2})$	Micro strain ε $\times 10^{-3}$	No.of crystalline per unit cell
Ag	0.221	41.23	0.0005	2.811	0.001
CFP	27.32	0.321	8.920	346.2	3008.1
Ag (1%)-CFP	5.093	1.726	0.309	64.53	514.1
Ag (3%)-CFP	1.531	7.346	0.0280	19.39	0.252
Ag (5%)-CFP	0.730	12.54	0.006	9.256	0.050

value a = 4.076 A° and the diffraction pattern is in good agreement with the literature report JCPDS File No. 04-0783. The well-defined intense peaks in diffraction pattern confirm excellent crystallinity of silver nanoparticles. Fig. 4b depicts the XRD pattern for CFP, which suggests that the polymer has amorphous structure. Fig. 5c-e represents the XRD patterns for Ag-CFP in 1%, 3% and 5% of silver intercalated in the CFP polymer, and one can see the peaks corresponding to the Ag crystallites. However, these peaks are slightly shifted, from their respective standard positions, may be due the presence of CFP polymer matrix. In addition, we observed reduced intensity of the peaks, and relatively larger peak broadening, compared with XRD of pure Ag nanoparticles. This indicates still smaller average size of Ag crystallites in composite polymer, compared to that of pure Ag nanoparticle. This suggests that Ag is present in the CFP polymer and the presence of CFP has influenced the preferred orientation of Ag nanoparticle in the polymer nanocomposites to some extent. The increase in the average crystallite size and an increase in the average dislocation density with the increase of Ag content into the CFP nanocomposites have been observed and presented in Table 1. This change in structural parameters clearly reveals that the Ag nanoparticles strongly interacted with CFP random copolymer. The average crystallite size (D) was evaluated from the FWHM of the diffraction peak using Scherer'sequation

$$D = 0.9\lambda / \beta \cos\theta \quad (1)$$

where β is the FWHM of the diffraction line in radians and λ is the X-ray wavelength. The calculated average crystallite sizes were found to be in the range of 0.3-42 nm and are listed in Table 1. The micro strain (ε), dislocation density (δ) and number of crystallites per unit area (N) were calculated using the following relations (Eqs. 2, 3 and 4) and their values are given inTable1.

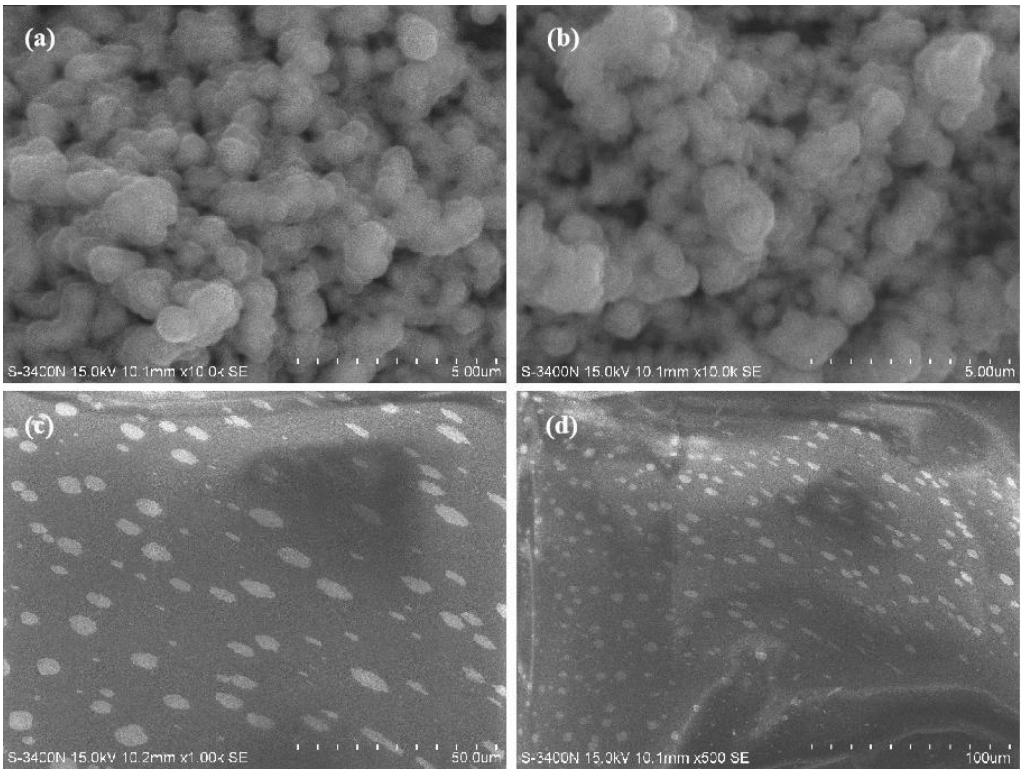

Fig. 6. SEM images of (a & b) Ag nanoparticle and (c & d) Ag (5%) –CFP.

Micro strain (ε) = β cosθ/4 (2)

Dislocation density (δ)= 15ε/*aD* *(3)*

Number of crystallites (N)=t/D^3 (4)

where θ is the Bragg's angle; t is thickness of the nanocomposites; ε is the strain that induces a deformation of one part per million.

SEM analysis

Morphology of the synthesized silver nanoparticles in the CFP polymer was observed from the SEM micrographs. Figs. 6(a-b), shows the SEM images of silver nanoparticles in spherical shape. The nanoparticles were not in direct contact even within the aggregates, indicating stabilization of the nanoparticles by a capping agent [50]. The larger silver particles may be due to the aggregation of the smaller ones, due to the SEM measurements. The SEM images of Ag (5%) -CFP composites (Fig. 5c-d) confirm that the Ag 5% nanoparticles are uniformly dispersed in CFP polymer matrix.

TEM analysis

The TEM images of Ag nanoparticles are in shown Fig.7a and 7b, which confirms that the Ag nanoparticles are spherical in shape. It is also observed that few agglomerates of small grains and some dispersed nanoparticles are seen. Further, silver nanoparticle is found to be in spherical shape (Fig. 7b.) and the particle size ranges from 10 to 50 nm with mean the average diameter of 25 nm.

Electrochemical characterization ofAg-CFP CyclicVoltammetry

Fig. 8 shows the electrochemical characterization of modified electrodes, oxidation and reduction peaks of CFP and the incorporation of 1% of Ag nanoparticles in CFP is clearly seen, the slight increase in redox peak may be due to the inhibition of electron transfer. However, higher loading of silver nanoparticles (Ag 5%-CFP) resulted in increased redox peak which may be due to the formation of conductive networks in the polymer matrix. The oxidation peak of Ag NPs appears at about +1.6 V versus reference electrode corresponding to a reverse reduction peak potential at -0.3 V versus reference electrode. The highest peaks observed from the AgNPs

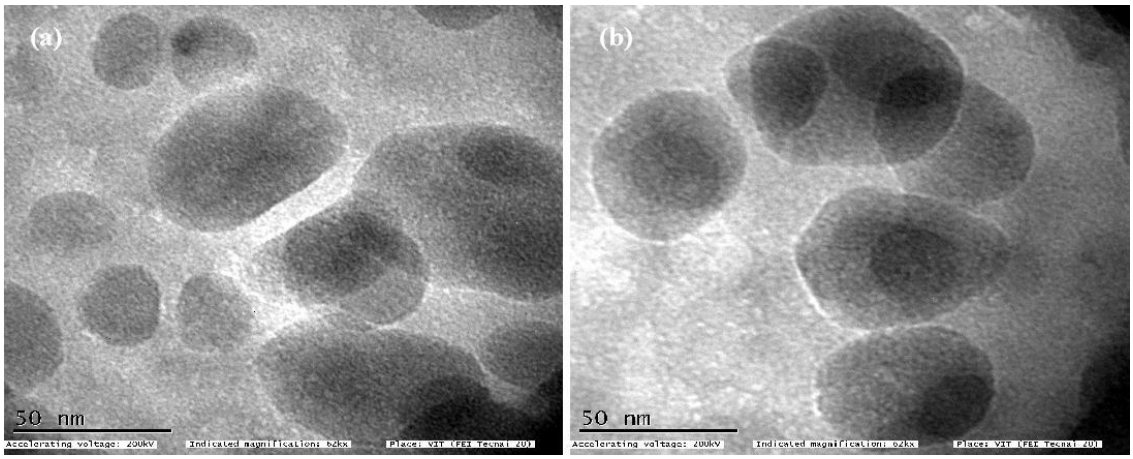

Fig.7. (a & b) TEM images of Ag nanoparticles.

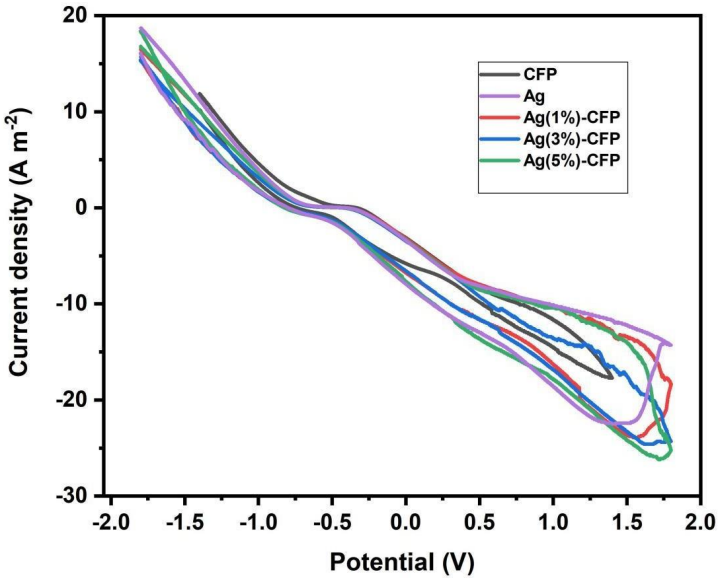

Fig. 8. The CV of CFP, Ag, Ag (1%)-CFP, Ag (3%)-CFP and Ag (5%)-CFP in PBS (pH7.0) at 100 mVs^{-1} scan rates.

composites indicate that the Ag (5%)-CFP has the strongest ability of enhancing electron transfer among the others. This might be due to the Ag NPs which can increase the conductivity of the film by facilitating the electron transfer. It is also evident from Fig 8 that the response current also increased proportionally to Ag content.

EIS studies

The Nyquist diagrams determined for Ag, CFP, Ag (1%)-CFP, Ag (3%)-CFP and Ag (5%)- CF-PareshowninFig.9(a),whileFig.9(b)displaysthecor-respondingBodeplots.The magnitude of the impedance indicates the surface resistance to transportation of electrons and charges. The impedance of the Ag (5%)-CFP composite is several folds smaller than the impedance of Ag, CFP, Ag (1%)-CFP and Ag (3%)-CFP implying increased charge/electron transfer via the Ag NPs. Such improvement in the charge/electron transfer would be beneficial to improve sensing ability. In EIS, the absolute value of the impedance is inversely proportional to capacitance and reduced impedance at low frequency implying an increase of electrochemical capacitance. In addition, electron/charge-transfer composite can be identified

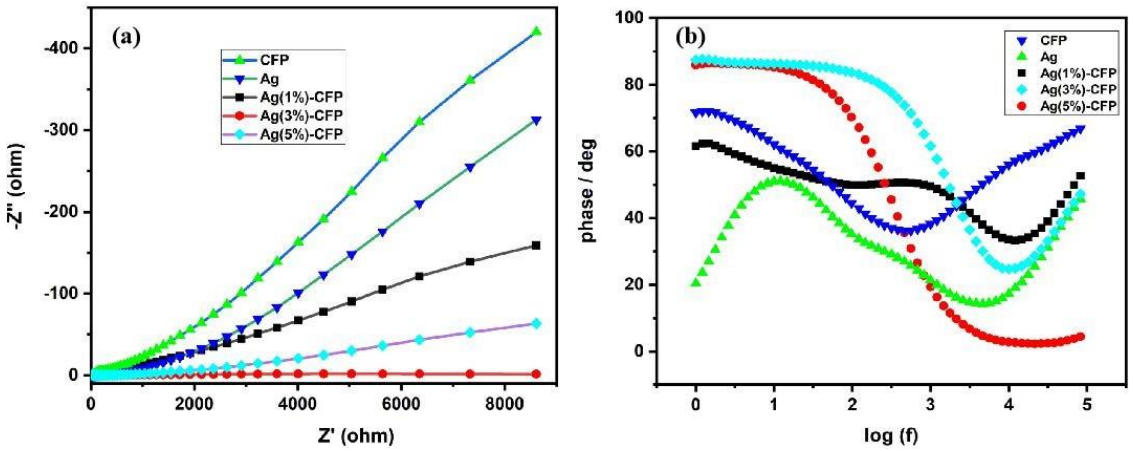

Fig. 9. (a) Electrochemical properties of the fabricated electrodes. The EIS studies of Ag, CFP, Ag (1%)-CFP, Ag (3%)-CFP, and Ag (5%)-CFP in0.1M PBS (pH 7.0) at 100mVs^{-1} scan rates. 8(b) Blot plot of Ag, CFP, Ag (1%)-CFP, Ag (3%)-CFP, and Ag (5%)-CFP.

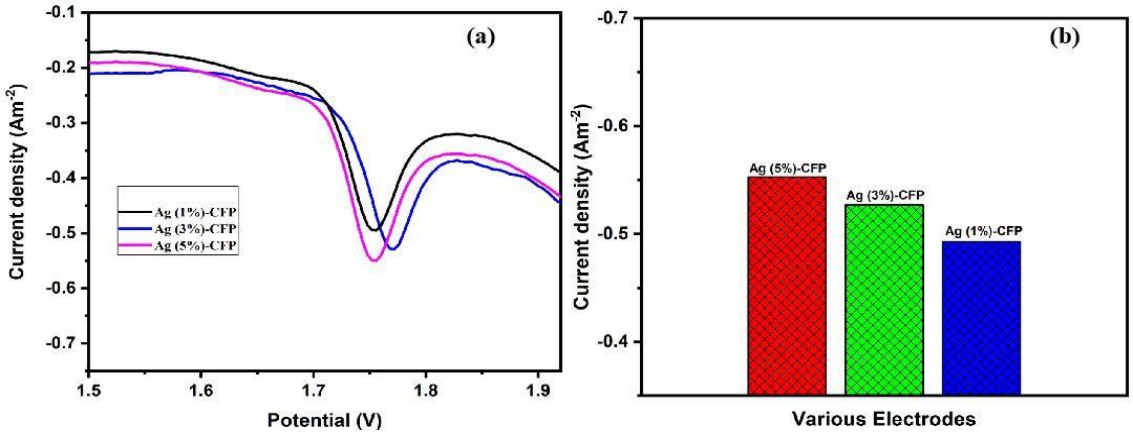

Fig. 10. (a) Electrochemical properties of the fabricated electrodes. The DPV studies of various electrodes in Ag, CFP, Ag(1%)-CFP, Ag(3%)-CFP, and Ag(5%)-CFP in0.1M PBS (pH 7.0) at 100 mVs-1 scan rate, (b) sensitivity of the electrodes.

from the phase angle expression of the Bode plots in Fig. 9(b). The phase angle of the Ag has two phases obtained at 52° and 19° and CFP has only one phase value at 42° after the formation of CFP composite with various weight percentage of Ag such as 1% 3% and 5%. The corresponding phase value that shifted to 42° 28° and 10° confirms the uniform dispersion of Ag in polymer matrix.

Differential Pulse Voltammetry

Fig. 10a shows the DPV behaviour of Ag-CFP modified ITO in the presence of 0.1 M PBS as supporting electrolyte. The enhanced peak current was observed for Ag (5%)-CFP when compared with various weight percentages of 1%, 3% of Ag-CFP under the experimental conditions. The 5% of Ag-CFP reduction peak current was larger than the 1% and 3% Ag- CFP electrode which can increase the conduction pathways and is anticipated to promote the electron transfer between the solution and electrode surface. The plot of the current density vs.

the various electrode is plotted in Fig. 10b, which also indicates that the Ag(5%)-CFP electrode exhibits high current density values when comparted to Ag (1%)-CFP and Ag(3%)-CFP electrodes. It is anticipated that Ag (5%)-CFP electrode may show enhanced sensitivity for DNA detection and which has been used for DNA hybridization studies.

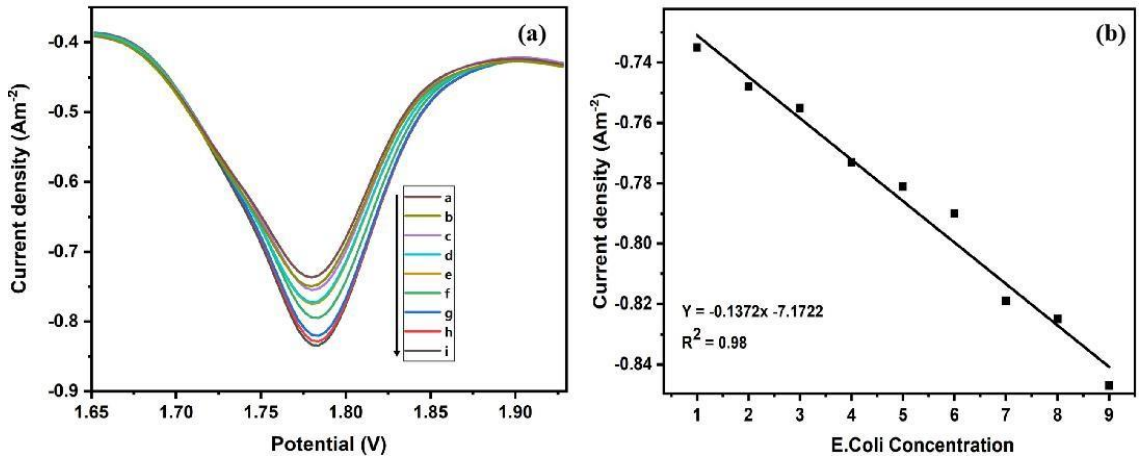

Fig.. 11. a) Evaluation of sensitivity of biosensor on a different *E.Coli* concentration of DPV response (a) pDNA/Ag(5%)-CFP/GCE, (b) 1 × 10^{-15} M, (c) 1 × 10^{-16} M, (d) 1 × 10^{-17} M (e) 1 × 10^{-18} M, (f) 1 × 10^{-19} M, (g) 1 × 10^{-20}M (h)1 × 10^{-21} M, (i) 1 × 10^{-22} M, in 0.1 M PBS at PH 7.0. b) The graph depicts linear relationship between current density and *E. Coli* concentration (logarithm).

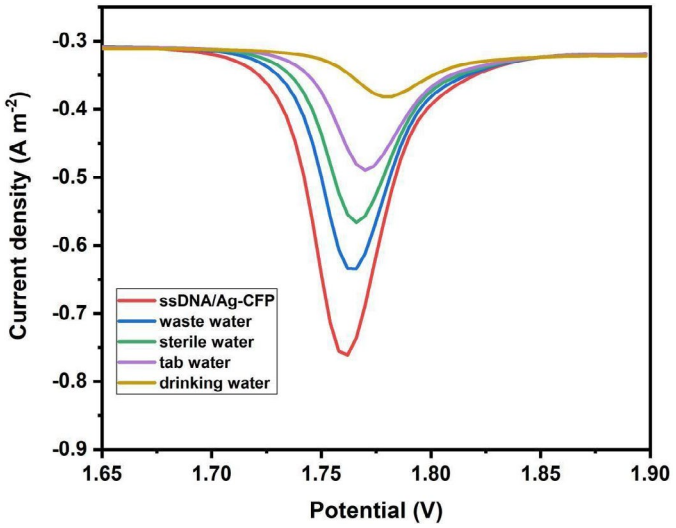

Fig. 12. DPV comparison between *E.Coli* detection in different water samples with ssDNA/Ag-CFP/ITO.

Bio sensing Studies

The working electrode used in Ag (5%)- CFP was also used for DNA sensor studies. Differential pulse voltammetry (DPV) experiments were performed in 0.1M Phosphate buffer solution (pH = 7) and experimental parameters were optimized according to the voltammetry response of Ag (5%)-CFP in the electrode surface. It has been observed that the peak current after hybridization was very low for tDNA/Ag (5%)-CFP/ITO bioelectrode showing maximum hybridization efficiency of tDNA with pDNA /Ag(5%)-CFP/ITO bioelectrode. Further, various tDNA of concentrations (1 × 10^{-15} to 1 × 10^{-22} M) were used for the biosensing studies at 25^{O}C in Fig.11 (a). On observation it is clear that incubation time of 60 s is sufficient for the interaction of ssDNA with tDNA bioelectrode as discussed earlier. As indicated in Fig. 11a, current signal of ssDNA/Ag (5%) - CFP/ITO decreases as the target concentration increases and remains constant with further increase in the tDNA concentration after incubation with tDNA sequence, which shows that the entire immobilized tDNA is involved in hybridization process at the bioelectrode surface. Fig. 11b indicates that the peak current of ssDNA/Ag (5%)-

CFP reduction follows linear relationship with a correlation coefficient of 0.98. The detection limit of the sensor is 1×10^{-22}M. The obtained results are comparable with literature reports on *E.coli* detection using DPV technique [51-53].

Water samples analysis

Fig. 12 shows the response of the biosensor with real water samples, such as drinking water, tap water, sterile water and waste water which are spiked with tDNA, exhibited a positive response to the presence of different concentration of *E. Coli* DNA. The results obtained in this water sample analysis were comparable to the standard graph obtained in Fig. 11(a). This biosensor showed better recyclability illustrating its applicability for water sample analysis.

CONCLUSION

In this work the potential of Ag nanoparticles loaded poly (9,9-dioctylfluorene-ran- phenylene) nanocomposites on the sensitive and specific electrochemical detection of ssDNA of *E. coli* has been studied. The oligonucleotide (pDNA) functionalized Ag-CFP electrode exhibited good sensitivity for the detection of ssDNA of *E. coli* through differential pulse volammetry measurements. Electrochemical studies demonstrated the successful pDNA immobilization and the hybridization of tDNA as monitored by DPV. In summary, we have employed a new conductive polymer embedded with Ag nanoparticle for the detection of *E.coli*, which showed a significant detection of the ssDNA of *E.coli* in the concentration range of 1×10^{-15} M to 1×10^{-22} M with a lowest detection of 1×10^{-22} M.

ACKNOWLEDGMENT

The authors acknowledge the financial support from the Department of Science and Technology, Govt of India through grant EMEQ/2016/00049.

CONFLICTS OF INTEREST

The authors do not have any personal or financial conflicts of interest.

REFERENCES

[1] Tarr P. I., Bilge S. S., Vary J. C. J., Jelacic S., Habeeb R. L., Ward T. R., Baylor M. R., Besser T. E., (2000), A novel *Escherichia coli* O157 : H7 adherence conferring molecule encoded on a recently acquired chromosomal island of conserved structure*. Infect. Immun.* 68: 1400–1407.

[2] Tang H., Zhang W., Geng P., Wang Q., Jin L., Wu Z., Lou M., (2006), A new amperometric method for rapid detection of Escherichia coli density using a self-assembled monolayer-based bienzyme biosensor. *Anal Chim. Acta*. 562: 190–196.

[3] Hatosy S. M., Martiny A. C., (2015), The ocean as a global reservoir of antibiotic resistance genes. *Appl. Environm. Microbiol.* 81: 7593–7599.

[4] Moore D. F., Guzman J. A., Mc Gee C., (2008), Species distribution and antimicrobial resistance of enterococci isolated from surface and ocean water. *J. Appl. Microbiol.* 105: 1017–1025.

[5] Marti E., Jofre J., Balcazar J. L., (2013), Prevalence of antibiotic resistance genes and bacterial community composition in a river influenced by a wastewater treatment plant. *PLoS One.* 8: e78906.

[6] Ronald J. A., Brena M., Melissa M., (2002), Antibiotic resistance of gram- negative bacteria in rivers, United States. *Emerg. Infect. Dis. J.* 8: 713–715.

[7] Pang Y. C., Xi J. Y., Li G. Q., Shi X. J., Hu H. Y., (2015), Prevalence of antibiotic-resistant bacteria in a lake for the storage of reclaimed water before and after usage as cooling water. *Environm. Sci: Proc. Impacts.* 17: 1182–1189.

[8] Rosas I., Salinas E., Martínez L., (2015), Characterization of Escherichia *coli* isolates from an urban lake receiving water from a wastewater treatment plant in Mexico city: fecal pollution and antibiotic resistance. *Current Microbiol.* 71: 490–495.

[9] Blaak H., van Hoek A. H. A. M., Veenman C., (2014), Extended spectrum β- lactamase- and constitutively AmpC-producing *Enterobacteriaceae* on fresh produce and in the agricultural environment. *Int. J. Food Microbiol.* 168: 8–16.

[10] Rodriguez-Mozaz S., Chamorro S., Marti E., (2015), Occurrence of antibiotics and antibiotic resistance genes in hospital and urban waste waters and their impact on the receiving river. *Water Res.* 69: 234-242.

[11] Figueras M. J., Borrego J. J., (2010), New perspectives in monitoring drinking water microbial quality. *Int. J. Environ.* 7: 4179-4202.

[12] Shagun G., Vipan K., (2020), Development of environmental biosensors for detection, monitoring, and assessment. *Nanomater. Environm. Biotechnol*. 107-125.

[13] Serdyukov D. S., Tatiana N., Goryachkovskaya I. A., Mescheryakova S. V., Bannikova S. A., Kuznetsov O. P., Cherkasova V. M. P., Sergey E. P., (2020), Study on the effects of terahertz radiation on gene networks of *Escherichia coli* **by means of fluorescent biosensors.** *Biomed. Optics Express.*11: 5258-5273.

[14] Kumar M., Ghosh S., Nayak S., Das A., (2016), A recent advances in biosensor based diagnosis of urinary tract infection. *Biosens. Bioelectron.* 80: 497–510.

[15] Azimzadeh M., Rahaie M., Nasirizadeh N., Daneshpour M., Naderi- Manesh H., (2017), Electrochemical miRNA biosensors: The benefits of nanotechnology. *J Nanomed. Res*. 2: 36–48.

[16] KurunduHewage E. D., Spear D., Umstead T. M., Hu S., Wang M., Wong P. K., Chroneos Z. C., Halstead E. S., Thomas N. J., (2017), An electrochemical biosensor for rapid detection of pediatric bloodstream infections*. SLAS Technology (Translating Life Sciences Innovation).* 22: 616–625.

[17] Ma X., Jiang Y., Jia F., Yu Y., Chen J., Wang Z., (2014), An aptamerbased electrochemical biosensor for the detection

of *Salmonella. J. Microbiol. Methods.* 98: 94–98.
[18] Pernaut J. M., Reynolds J. R., (2000), Use of conducting electroactive polymers for drug delivery and sensing of bioactive molecules. A redox chemistry approach. *J. Phys. Chem*. *B.* 104: 4080–4090.
[19] Park S. M., (1997), Electrochemistry of π-conjugated polymers. In Handbook of Organic Conductive Molecules and Polymers, UK, 3: 429–469.
[20] Guiseppi-Elie A., Wallace G. G., Matsue T., (1998), Handbook of Conducting Polymers, 2nd ed. New York. NY. USA.963.
[21] Kim Y. H., Lee J., Hofmann S., Gather M. C., Müller-Meskamp L., Leo K., (2013), Achieving high efficiency and improved stability in ITO free transparent organic light-emitting diodes with conductive polymer electrodes. *Adv. Funct. Mater.* 23:3763–3769.
[22] Defieuw G., Samijn R., Hoogmartens L., Vanderzande D., Gelan J., (1993), Antistatic polymer layers based on poly(isothianaphthene) applied from aqueous compositions. *Synth. Met.* 57: 3702–3706.
[23] Shen K. Y., Hu C. W., Chang L. C., Ho K. C., (2012), A complementary electrochromic device based on carbon nanotubes/conducting polymers. *Sol. Energy Mater. Sol. Cells.* 98: 294–299.
[24] Mengistie D. A., Ibrahem M. A., Wang P. C., Chu C. W., (2014), Highly conductive PEDOT: PSS treated with formic acid for ITO-free polymer solar cells. *ACS Appl. Mater. Interfaces.* 6: 2292–2299.
[25] Baldissera A. F., Freitas D. B., Ferreira C. A., (2010), Electrochemical impedance spectroscopy investigation of chlorinated rubber-based coatings containing polyaniline as anticorrosion agent. *Mater. Corros.* 61: 790–801.
[26] Rahman M.M., Li X. B., Jeon Y. D., Lee H. J., Lee S. J., Lee J. J., (2012), Simultaneous determination of ranitidine and metronidazole at poly(thionine) modified anodized glassy carbon electrode*. J. Electrochem. Sci. Technol*. 2: 90–94.
[27] Svirskis D., Travas-Sejdic J., Rodgers A., Garg S., (2010), Electrochemically controlled drug delivery based on intrinsically conducting polymers. *J. Control. Release.* 146: 6–15.
[28] Leprince L., Dogimont A., Magnin D., Champagne S. D., (2010), Dexamethasone electrically controlled release from polypyrrole-coated nanostructured electrodes. *J. Mater. Sci. Mater. Med.* 21: 925–930.
[29] Kim J. S., Friend R. H., Cacialli F., (1999), Electrochemical and luminescent properties of poly (fluorene) derivatives for optoelectronic applications. *Appl. Phys. Lett.* 74: 3084-3089.
[30] Dhand C., Das M., Datta M., Malhotra B., (2011), Recent advances in polyaniline based biosensors. *Biosens Bioelectron*. 26: 2811–2821.
[31] Daneshpour M., Izadi P., Omidfar K., (2016), Femtomolar level detection of RASSF1A tumor suppressor gene methylation by electrochemical nano-genosensor based on Fe_3O_4/TMC/Au nanocomposite and PT-modified electrode. *Biosens Bioelectron*. 77: 1095– 1103.
[32] Poonam V., Sanjiv Kumar M., (2019), Applications of Silver nanoparticles in diverse sectors. *Int. J. Nano Dimens.* 10:18-36.
[33] Hadi B., Mohadeseh S., Somayeh T., (2019), Application of Graphene and Graphene Oxide for modification of electrochemical sensors and biosensors: A review. *Int. J. Nano Dimens.* 10: 125-140.
[34] Kwon O. S., Park S.J., Hong J. Y., Han A. R., Lee J. S., Oh J. H., Jang J., (2012), Flexible FET-type VEGF aptasensor based on nitrogen-doped graphene converted from conducting polymer. *ACS Nano*. 6: 1486–1493.
[35] Chen A., Chatterjee S., (2013), Nanomaterials based electrochemical sensors for biomedical applications. *Chem. Soc. Rev.* 42: 5425-5438.
[36] Saptarshi D., Kumar Das C., (2017), Silver nanoparticles decorated polypyrrole/graphene nanocomposite: a potential candidate for next-generation supercapacitor electrode material. *J. Appl. Polym. Sci.* 133: 44724.
[37] Tahira A., MohdShahanbaj K., Hemalatha S., (2018), A facile and rapid method for green synthesis of Silver Myco nanoparticles using endophytic. *Int. J. Nano Dimens.* 9: 435-441.
[38] Abdullah H., Mohammad Naim N., Azmy N. A. N., Abdul Hamid A., (2014), PANI- Ag-Cu Nanocomposite Thin Films Based Impedimetric Microbial Sensor for Detection of *E. Coli* Bacteria. *Anal. Methods*. 1 - 8.
[39] Zheng W., He L., (2009), Label-free, real-time multiplexed DNA detection using fluorescent conjugated polymers. *J. Am. Chem. Soc*. 131: 3432–3433.
[40] Kushon S. A., Ley K. D., Bradford K., Jones R. M., McBranch D., Whitten D., (2002), Detection of DNA hybridization via fluorescent polymer superquenching. *Langmuir.* 18: 7245-7249.
[41] Suria M. S., Jaafar A., Suraya A. R., Yap W. F., Faridah S., Lau H. Y., (2020), A carbon dots based fluorescence sensing for the determination of *Escherichia coli* O157 : H7. *Measurement*. 160: 107845-107852.
[42] Miaolin D., Xiaoyue X., Yanmei H., Guoqiang L., Shan S., Xi L., Houde Z., Silu P., Chengwei L., Daofeng L., Weihua L., (2021), Immuno-HCR based on contact quenching and fluorescence resonance energy transfer for sensitive and low background detection of *Escherichia coli* O157 : H7. *Food Chem*. 334: 127568-127573.
[43] Srinivasan K., Thiruppathiraja C., Saroja V., Kamatchiammal S., (2014), Dual labeled Ag@SiO_2 Core-Shell nanoparticles based optical immuno sensor for sensitive detection of *E. coli. Mater. Sci. Eng. C*. 45: 337-342.
[44] Xiaoyan Z., Tingting W., Yuemeng Y., Yongqiang W., Shutao W., Li-Ping X., (2020), Superwettable electrochemical biosensor based on a dual-DNA walker strategy for sensitive *E. coli* O157 : H7 DNA detection. *Sens. Actuators B: Chem*. 321: 128472-128479.
[45] Maribel G., Guzmán H., Jean D., Stephan G., (2009), Synthesis of silver nanoparticles by chemical reduction method and their antibacterial activity. *Int. J. Chem. Biomolec. Eng*. 2: 3-9.
[46] Puthiaraj P., Kim S-S., Ahn W-S., (2015), Covalent triazine polymers using a cyanuricchloridepreсursor via Friedel-Crafts reaction for CO_2 adsorption/separation. *Chem. Eng. J.* 11-15.
[47] Niraimathi K. L., Sudha V., Lavanya R., Brindha P., (2013), Biosynthesis of silver nanoparticles using Alternanthera sessilis (Linn.) extract and their antimicrobial, antioxidant activities. *Colloids and Surf. B: Biointerf.* 102: 288-291.
[48] Prakash P., Gnanaprakasam P., Emmanuel R., Arokiyaraj S., Saravanan M., (2013), Green synthesis of silver nanoparticles from leaf extract of Mimusopselengi, Linn. for enhanced antibacterial activity against multi drug resistant clinical isolates. *Colloids and Surf. B: Biointerf.* 108: 255-259.

[49] Dubey S. P., Lahtinen M., Sillanpaa M., (2010), Tansy fruit mediated greener synthesis of silver and gold nanoparticles. *Proc. Biochem.* 45: 1065-1071.
[50] Priya A. M., Selvan R. K., Senthilkumar B., Satheeshkumar M. K., Sanjeeviraja C., (2011), Synthesis and characterization of $CdWO_4$ nanocrystals. *Ceram. Int.* 7: 2485–2488.
[51] Sharma A., Pandey C. M., Matharu Z., Soni U., Sapra S., Sumana G., Pandey M. K., Chatterjee T., Malhotra B. D., (2018), Nanopatterned cadmium selenide Langmuir–Blodgett platform for leukemia detection. *Anal. Chem.* 84: 3082-3089.
[52] Zhu N., Chang Z., He P., Fang F., (2016), Electrochemically fabricated polyaniline nanowire-modified electrode for voltammetric detection of DNA hybridization. *Electrochim. Acta*. 51: 3758-3762.
[53] Pangajam A., Theyagarajan K., Dinakaran K., (2020), Highly sensitive electrochemical detection of *E. coli* O157 : H7 using conductive Carbon dot/ZnO nanorod/PANI composite electrode. *Sensing and Biosens. Res.* 29: 100317-100323.